Nucleophilic Reactivation of Sarin-Inhibited Acetylcholinesterase: A Molecular Modeling Study

Reinaldo T. Delfino and José D. Figueroa-Villar*

Seção de Engenharia Química, Instituto Militar de Engenharia, Praça Gen Tibúrcio, 80, Praia Vermelha, 22290-070, Rio de Janeiro - RJ, Brazil

Received: December 04, 2008; Revised Manuscript Received: March 26, 2009

Oximes have been used as reactivators for organophosphorus-inhibited acetylcholinesterase (AChE). However, it is still not clear why oximes are more efficient than other nucleophiles, since the reactivation consists of a simple nucleophilic substitution. In an attempt to answer this question, we have modeled the sarin-inhibited AChE reactivation by other nucleophiles (with and without the so-called α-effect) by applying the B3LYP/6-311G(d,p) level of theory. We have concluded that oximes reactivate AChE by a three-step mechanism in opposition to the four-step processes of the other modeled nucleophiles. In addition, our model suggests that oximes react with AChE in the deprotonated form (oximate). Our results also indicate that other nucleophiles may be used as AChE reactivators. We propose the use of hydrazones and hydrazonates for further evaluation as antidotes for intoxication by chemical warfare agents.

Introduction

Acetylcholinesterase (AChE, E.C. 3.1.1.7) is a serine hydrolase whose main function is to terminate nervous impulse transmission by hydrolysis of the cationic neurotransmitter acetylcholine (ACh).[1,2] This hydrolysis occurs near the bottom of an active site gorge, containing a catalytic triad composed of a nucleophilic serine, a hystidine, and a glutamate (Ser-200, Hys-440, and Glu-327 in *Torpedo californica* AChE,[3−7] Ser-203, Hys-447, and Glu 334 in human AChE[7]). ACh-mediated neurotransmission is a vital process for survival, and an inhibitor that binds to the serine at the active site prevents AChE from performing its catalytic function, resulting in several deleterious effects (including death).

Organophosphorus compounds are known to possess anticholinesterase activity, inhibiting AChE by establishing a covalent bond between its phosphorus atom and the alcoholic oxygen of the serine at the active site. Phosphylated AChE ("phosphylation" meaning both "phosphorylation" and phosphonylation") can no longer hydrolyze ACh and is much more stable than acetylated AChE; depending on the groups attached to the phosphorus atom, inhibition of AChE can be irreversible.[3,8−12] Because of their anticholinergic action, organophosphorus compounds have been used as insecticides and as chemical war agents (nerve agents).[13,14] The confirmed use of tabun, sarin, and VX in wars, localized conflicts, and terrorist attacks[15−23] shows that nerve agents constitute a threat that should not be underestimated.

Oximes have been used to reactivate AChE inhibited by organophosphorus compounds, regenerating its catalytic activity.[19,24] Several recent studies conducted by Wang and co-workers brought some insights into the mechanisms of AChE inhibition by organophosphorus compounds and its reactivation by oximes.[25−27] First, they studied simplified models of AChE phosphonylation by sarin in gas phase and in solution concluding that the reaction occurs through a two-step addition−elimination mechanism, rather than a concerted one.[25] Then, they have modeled the reactivation of sarin-inhibited AChE by formoximate, also through an addition−elimination mechanism, and have proposed that the reaction can occur easily in gas phase and in water due to the low energy barriers of the process.[26] Finally, they have studied a more sophisticated model of the AChE-inhibition by sarin, concluding that the rate-determining step of the addition−elimination mechanism would be the first one (the addition of the nerve agent to AChE).[27]

An oxime should have some structural properties for being an efficient AChE reactivator.[28,29] However, to our knowledge, it is not clear why only oximes are used as reactivators; since AChE reactivation involves just a nucleophilic substitution, in principle any nucleophile should work as reactivator (limited, of course, by clinical considerations, such as pharmacokinetics and toxicity of the compound). The only possible explanation we have found in the literature regards to the so-called α-effect,[30,31] which increases the nucleophilicity of oximes and oximates. But again, some questions arise. Should all AChE reactivators present an α-effect? Could an α-nucleophile that is not an oxime be used as reactivator? If not, why? If yes, then which nucleophiles would be the most efficient reactivators?

In an attempt to answer these questions, we have modeled the reactivation of a sarin-serine adduct model by different nucleophiles, all of them related to formoximate. This study was accomplished using a very simplified model of the serine dephosphylation reaction, corresponding to a nonenzymatic procedure. The would-be mechanisms of reaction and potential energy surfaces were investigated with the aid of density functional theory (DFT) calculations. The results obtained in the gas phase model and in polarizable continuum aqueous solvation model (PCM) suggest that, in theory, other nucleophiles may be used as AChE reactivators, and that hydrazones and hydrazonates should be further evaluated for use as antidotes.

We have also modeled reactivation by the neutral formoxime in order to discover which is the preferred form of the oxime for the reaction, the deprotonated[32] or the protonated one.[33] The obtained theoretical energy profiles suggest that, in the modeled

* To whom correspondence should be addressed. E-mail: figueroa@ime.eb.br.

10.1021/jp810686k CCC: $40.75
Published on Web 05/18/2009

conditions, the deprotonated form (the oximate) is indeed the active one for reactivating AChE.

Methods

This work was based on the model of the sarin-serine adduct reactivation by formoximate proposed by Wang and co-workers, and most of the used procedures were similar to the ones described in their work.[26] All calculations were performed using the DFT with the Becke's 3-parameter (B3) exchange functional[34] and the Lee, Yang, and Parr (LYP) nonlocal correlation functional[35,36] (B3LYP model). The basis set in all cases was the 6-311G(d,p), that is, the split valence triple-ζ basis set augmented with d polarization functions on heavy atoms and p polarization functions on hydrogen atoms.[37,38]

All minima in the potential energy surface corresponding to the studied reactions (reagents, intermediates, and products) were found by minimization, and their harmonic frequencies were verified to be real. The structures of the transition states were also found by minimization, and for each one of them it was confirmed the existence of just one imaginary harmonic frequency. The proposed connections among transition states and adjacent minima (the reaction pathways) were confirmed by the use of intrinsic reaction coordinate (IRC) analysis. Atomic charges were calculated by natural bond orbital analysis[39] at the same theoretical level. The PCM[40−44] with a dielectric constant of 78.39 (corresponding to water) was applied to all optimized minima and transition states in order to evaluate the solvation effects on the reaction pathways. This approximation is justified by the usually general fact that the use of gas-phase optimized structures with solvation energy corrections generates potential energy surfaces very similar to the ones obtained by optimization in solution.[45,46] Single point energy calculations with the B3LYP/6-311+G(d,p) level of theory were performed in all stationary points obtained in this work.

All described calculations were carried out with the Gaussian 03 package.[47]

Results and Discussion

We have applied an analogous procedure to that described by Wang and co-workers[26] in order to evaluate the effect of changing the nucleophile in the reactivation reaction and to compare our results with those published in the literature.[26] In this way, we chose to model reactivations by an enolate (which does not present an α-effect), a peroxile, a sulfenate (both of which do have an α-effect), and a hydrazonate (which contains a different nucleophilic atom). It is important to make clear that some of the chosen nucleophiles, due to the difficulty to generate them in physiological conditions, may not have potential practical use as antidotes, and that this study is focused on the understanding of the effect of the nucleophilic nature of those compounds on dephosphylation reactions. Wang's group chose a modeled sarin-serine adduct, represented in Chart 1, to emulate AChE's active site (which corresponds to the model of a nonenzymatic reactivation) and the simplest oximate, formoximate, to model the role of the oximes in its reactivation. In the model of the sarin-serine adduct, the sarin's isopropyl is replaced by a methyl group to reduce the computational cost. We have chosen the following nucleophiles that are structurally analogous to the formoximate: the acetaldehyde enolate, methylperoxile, methylsulfenate, formaldehyde hydrazonate, and the neutral formoxime, whose structures are also represented in Chart 1.

The model for the adduct's reactivation by formoximate, proposed by Wang's group,[26] consists of a three-step mechanism. The first step is the nucleophilic attack of the oximate, concerted with a rotation of the serine bound to sarin; the second step is a very low energy barrier rotation of the sarin methoxyl group, which directs itself toward the serine; and the last step is the elimination of the serine as a leaving group. The energy barrier of the second step is so low that the authors consider the reaction to be a two-step addition−elimination mechanism. Their work proposes that in the gas phase the first step is the rate-limiting one, while the third step is the rate-limiting one in aqueous solution.

CHART 1: Structures of the Sarin-Serine Adduct, the Formoximate, and the Nucleophiles Used in This Work

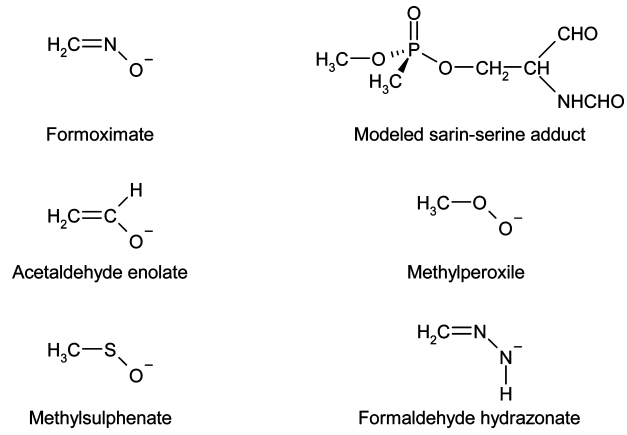

By applying the same procedure to model the hypothetical serine reactivations by the acetaldehyde enolate, methylperoxile, methylsulfenate, and formaldehyde hydrazonate, we have modeled possible pathways for these reactions. However, we have not been able to model a three-step mechanism for any of them; all proposed reaction paths have four steps. The stationary points found in the potential energy surface of each reactivation are shown in Figures 1 to 4. Tables 1 to 4 list the energy properties of these states.

The modeled reactions pathways for reactivations by the enolate, the peroxile, and the sulfenate are quite similar, as can be seen in Figures 1 to 3. The major difference among them is the relative position of the nucleophile in the first minimum (INT_1) and in the first transition state (TS_1). Although our models do not give any clue for the reason of this difference, they indicate that the correct orientation of the nucleophile is essential for the nonenzymatic reaction itself, not being only a constraint imposed by the shape of the active site of AChE. Wang and co-workers reached the same conclusion for reactivation by formoximate.[26]

When compared to the three-step mechanism of reactivation by formoximate, it is clear that the mechanisms for those three nucleophiles distinguish themselves at the beginning of the reaction. For formoximate, the first transition state of the reaction involves a nucleophilic attack concerted with a rotation of the serine, while for the other nucleophiles these two processes take place separately. First, there occurs the nucleophilic attack, and just after passing through a new intermediate (not observed in the formoximate reaction) there occurs the serine rotation. The last two steps are analogous to the ones observed in the reactivation by formoximate: the rotation of the methoxyl group and the liberation of the serine. In order to keep a similar nomenclature to the one employed by Wang's group,[26] we decided to designate the first, third, and last transition states as TS_1, TS_2, and TS_3, respectively, since they correspond to processes analogous to the observed in their model. The second and new transition state, corresponding to the rotation of serine,

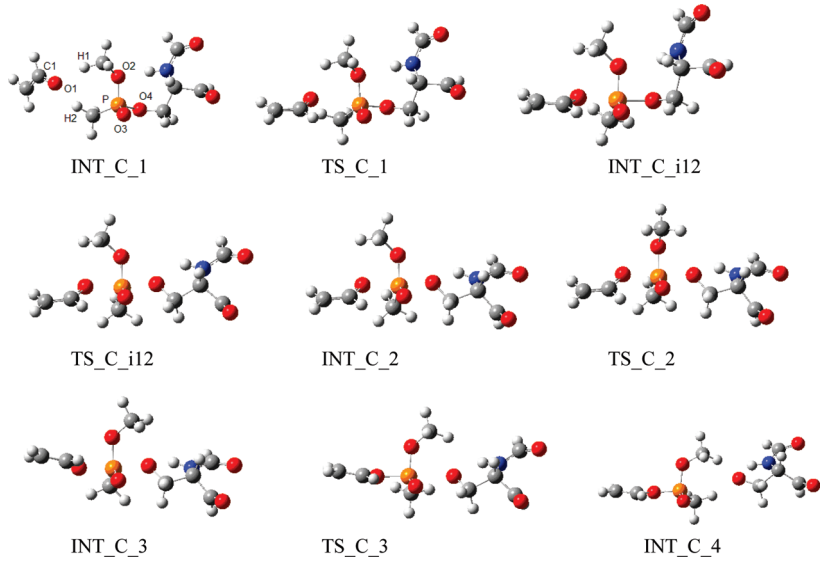

Figure 1. Structures of the minima (INT_C) and transition states (TS_C) of the potential energy surface of the modeled sarin-serine adduct reactivated by acetaldehyde enolate, obtained by B3LYP/6-311G(d,p) (C in gray, O in red, N in blue, P in orange, and H in white).

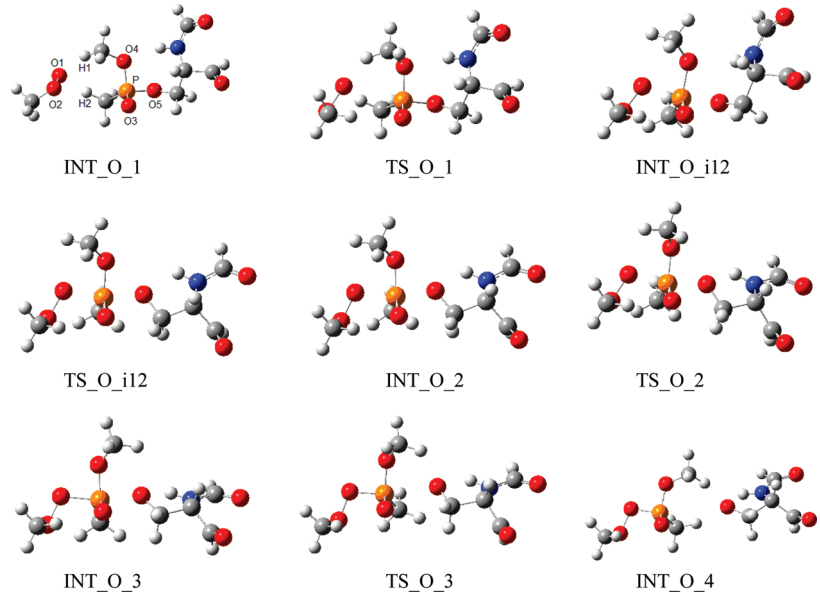

Figure 2. Structures of the minima (INT_O) and transition states (TS_C) of the potential energy surface of the modeled sarin-serine adduct reactivated by methylperoxile, obtained by B3LYP/6-311G(d,p) (C in gray, O in red, N in blue, P in orange, and H in white).

has been designated as TS_i12 (that is, a new transition state located in an intermediate position between TS_1 and TS_2). Minima in the potential energy surface (INT) have been designated accordingly. An additional letter placed between the letters indicating the stationary point (INT or TS) and the number refers to the modeled nucleophile, as shown in Figures 1 to 4.

To summarize the results for reactivations by acetaldehyde enolate, methylperoxile, and methylsulfenate, it can be said that they occur through a four-step mechanism. In each case, the vibrational mode of the imaginary frequency of the first transition state (73i cm^{-1} for TS_C_1, 103i cm^{-1} for TS_O_1, 106 cm^{-1} for TS_S_1) corresponds to the nucleophilic attack of the reactivator. For the second transition state of each reaction, the vibrational mode of the imaginary frequency (15i cm^{-1} for TS_C_i12, 8i cm^{-1} for TS_O_i12, 10i cm^{-1} for TS_S_i12) corresponds to rotation of the serine. The third transition state in each case has a vibrational mode for the imaginary frequency (72i cm^{-1} for TS_C_2, 71 cm^{-1} for TS_O_2, 72i cm^{-1} for TS_S_2) corresponding to the rotation of the methoxyl group toward the serine. Finally, the last transition state in each case has an imaginary frequency (88i cm^{-1} for TS_C_3, 78i cm^{-1} for TS_O_3, 96i cm^{-1} for TS_S_3) whose vibrational mode shows the departure of serine. It is noteworthy that all modeled transition states for the rotation of the serine (TS_i12) have low-module imaginary frequencies. This fact, associated to the low potential energy differences between these transition states and the following minima INT_2 (see Tables 1 to 3), demands some caution in considering their existence. However, the significant free energy differences between TS_i12 and INT_2 in each case and the inability in modeling three-step reaction pathways for these nucleophiles suggest that these transition states should actually exist.

As noted by one of the referees, the formation of sulfenates has been postulated in nucleophilic substitutions of phosphonothiolates, such as solvolysis of the VX-analogous O,S-dimethyl methylphosphonothiolate.[46] However, the formation of the sulfenate would be the result of a possible alternate

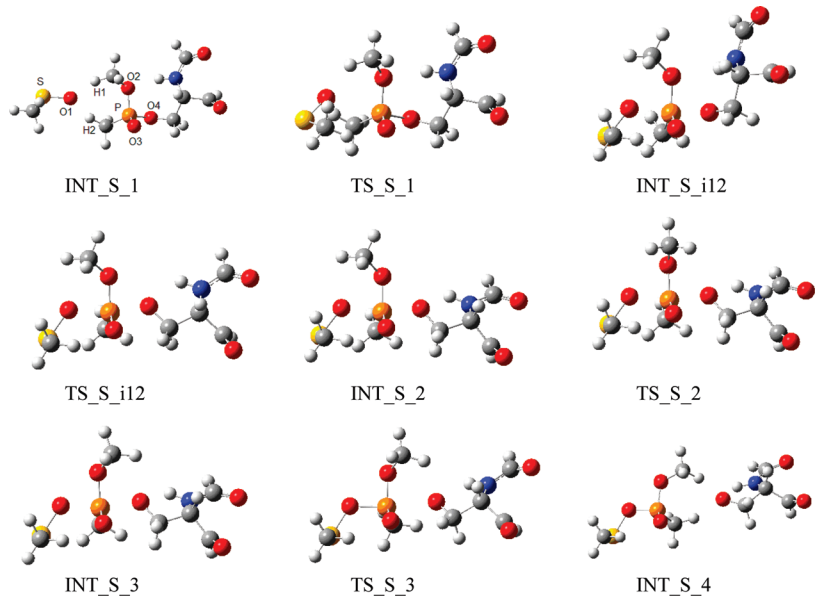

Figure 3. Structures of the minima (INT_S) and transition states (TS_S) of the potential energy surface of the modeled sarin-serine adduct reactivated by methylsulfenate, obtained by B3LYP/6-311G(d,p) (C in gray, O in red, N in blue, P in orange, H in white, and sulfur in yellow).

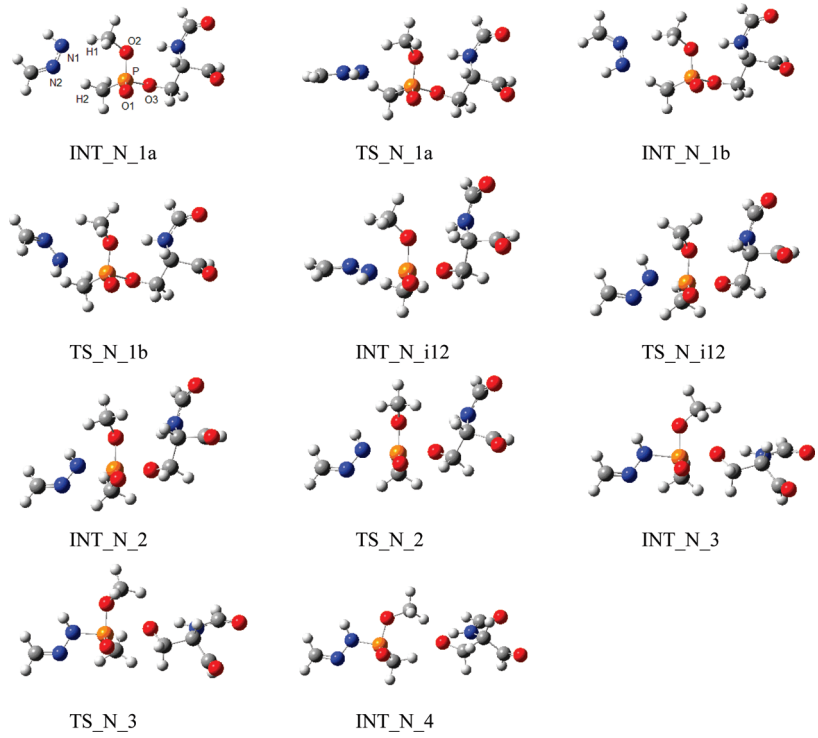

Figure 4. Structures of the minima (INT_N) and transition states (TS_N) of the potential energy surface of the modeled sarin-serine adduct reactivated by formaldehyde hydrazonate, obtained by B3LYP/6-311G(d,p) (C in gray, O in red, N in blue, P in orange, and H in white).

reaction pathway in the nucleophilic substitution mechanism, and it would not act as a nucleophile such as modeled in this work.

The modeled reactivation by formaldehyde hydrazonate presents many differences when compared to the previously described reaction pathways. First of all, we were able to model two distinct mechanisms for this process, which differ between themselves on the first minimum and on the first transition state. These stationary points can be seen in Figure 4 (designated as INT_N_1a and TS_N_1a for one of the possible mechanisms, and INT_N_1b and TS_N_1b for the other). The main difference between the two mechanisms is the relative position of the hydrazonate; in TS_N_1a, the torsional angle N2−N1−P−O3 is 22.6°, while in TS_N_1b the same angle is −59.4°. The IRC analysis indicates that both transition states TS_N_1a and TS_N_1b proceed to the INT_N_i12 minimum, and the remaining steps for both modeled pathways are the same. Table 4 shows that INT_N_1b is 0.8 kcal/mol more stable than INT_N_1a (with and without zero point energy correction, ZPE). However, the electronic energy barrier between INT_N_1a and TS_N_1a (1.8 kcal/mol without ZPE, 2.0 kcal/mol with ZPE) is lower than that between INT_N_1b and TS_N_1b (3.8 kcal/mol without ZPE, 4.0 kcal/mol with ZPE). The same phenomenon is observed when Gibbs free energy barriers are considered (4.2 versus 5.2 kcal/mol). These data lead us to conclude that

TABLE 1: Energies for Minima and Transition States of the Sarin-Serine Adduct Reactivation by Acetaldehyde Enolate at the B3LYP/6-311G(d,p) Level (kcal/mol)

structures	ΔE (without ZPE)[a]	ΔE (with ZPE)[a]	ΔG^0 (298.15 K)[b]	ΔE_{PCM}[c]
INT_C_1[d]	0.0 (−1161.67025)	0.0 (−1161.43643)	0.0 (−1161.49056)	0.0 (−1161.75913)
TS_C_1	4.1	4.2	6.2	4.8
INT_C_i12	−1.4	−0.3	2.3	4.1
TS_C_i12	2.4	3.1	6.2	6.8
INT_C_2	2.3	3.2	5.3	5.6
TS_C_2	4.1	4.6	7.6	8.0
INT_C_3	2.2	2.9	5.2	5.5
TS_C_3	5.1	5.0	6.5	11.2
INT_C_4	−0.1	−0.4	−0.5	6.4

[a] ZPE correction with scaling factor of 0.9877, recommended for the B3LYP/6-311G(d,p) level.[48] [b] Free energies calculated with scaling factor of 0.9877. [c] Energies calculated with PCM model, as described in Methods. [d] The energy differences are calculated based on the energy value of INT_C_1 (whose value, in hartrees, is listed in parentheses).

TABLE 2: Energies for Minima and Transition States of the Sarin-Serine Adduct Reactivation by Methylperoxile Enolate at the B3LYP/6-311G(d,p) Level (kcal/mol)

structures	ΔE (sem ZPE)[a]	ΔE (com ZPE)[a]	ΔG^0 (298.15 K)[b]	ΔE_{PCM}[c]
INT_O_1[d]	0.0 (−1198.70574)	0.0 (−1198.47308)	0.0 (−1198.52592)	0.0 (−1198.79704)
TS_O_1	4.3	4.1	4.8	4.0
INT_O_i12	−9.7	−8.6	−6.8	−4.8
TS_O_i12	−6.4	−5.7	−2.6	−2.4
INT_O_2	−6.5	−5.7	−4.2	−3.1
TS_O_2	−6.4	−5.7	−3.4	−2.8
INT_O_3	−7.8	−7.1	−6.0	−4.1
TS_O_3	−5.4	−5.7	−4.5	0.8
INT_O_4	−9.8	−10.3	−11.7	−2.4

[a] ZPE correction with scaling factor of 0.9877, recommended for the B3LYP/6-311G(d,p) level.[48] [b] Free energies calculated with scaling factor of 0.9877. [c] Energies calculated with PCM model, as described in Methods. [d] The energy differences are calculated based on the energy value of INT_O_1 (whose value, in hartrees, is listed in parentheses).

TABLE 3: Energies for Minima and Transition States of the Sarin-Serine Adduct Reactivation by Methylsulphenate at the B3LYP/6-311G(d,p) Level (kcal/mol)

structures	ΔE (without ZPE)[a]	ΔE (with ZPE)[a]	ΔG^0 (298.15 K)[b]	ΔE_{PCM}[c]
INT_S_1[d]	0.0 (−1521.76653)	0.0 (−1521.53589)	0.0 (−1521.59057)	0.0 (−1521.85372)
TS_S_1	4.5	4.6	6.4	4.3
INT_S_i12	−3.0	−2.3	0.2	1.0
TS_S_i12	0.8	0.9	4.2	3.7
INT_S_2	0.7	1.0	2.8	2.8
TS_S_2	1.8	1.8	4.7	4.2
INT_S_3	1.2	1.4	3.2	3.2
TS_S_3	3.3	2.5	3.9	7.6
INT_S_4	−2.6	−3.5	−3.8	2.3

[a] ZPE correction with scaling factor of 0.9877, recommended for the B3LYP/6-311G(d,p) level.[48] [b] Free energies calculated with scaling factor of 0.9877. [c] Energies calculated with PCM model, as described in Methods. [d] The energy differences are calculated based on the energy value of INT_S_1 (whose value, in hartrees, is listed in parentheses).

the reaction pathway initiated by INT_N_1a should have a slight preference over the other one.

Another remarkable difference in the mechanism of reactivation by the formaldehyde hydrazonate lies in the second step of the reaction. While the second step in the previously described reactivations corresponded to a rotation of the serine, in the case of hydrazonate this step correspond to a pronounced rotation of the nucleophile; the torsional angle N2−N1−P−O3 has values of −8.8° in INT_N_i12, 127.0° in TS_N_i12, and 134.5° in INT_N_2. The rotation of the serine group occurs in the third step (TS_N_3), concerted with the rotation of the methoxyl group.

The summary of the four-step reactivation by the formaldehyde hydrazonate is as follows: in the first step, the vibrational mode for the imaginary frequency of the transition state (66i cm^{-1} for TS_N_1a, 87i cm^{-1} for TS_N_1b) represents the nucleophilic attack of the hydrazonate to the phosphylated serine. The second step involves a transition state (TS_N_i12) whose imaginary frequency (122i cm^{-1}) has a vibrational mode showing an expressive rotation of the hydrazonate. Unlike the previous cases, the module of the imaginary frequency of the second step is not very low, so that we can consider this saddle point as well characterized. The reaction proceeds and reaches transition state TS_N_2, whose imaginary frequency (66i cm^{-1}) has a vibrational mode corresponding to the simultaneous rotations of the methoxyl group and the serine. Finally, the last step involves transition state TS_N_3, and the vibrational mode of its imaginary frequency (61i cm^{-1}) shows the departure of the serine from the phosphylated hydrazone.

TABLE 4: Energies for Minima and Transition States of the Sarin-Serine Adduct Reactivation by Formaldehyde Hydrazonate at the B3LYP/6-311G(d,p) Level (kcal/mol)

structures	ΔE (without ZPE)[a]	ΔE (with ZPE)[a]	ΔG^0 (298.15 K)[b]	ΔE_{PCM}[c]
INT_N_1a[d]	0.0 (−1157.78557)	0.0 (−1157.55206)	0.0 (−1157.60562)	0.0 (−1157.87326)
TS_N_1a	1.8	2.0	4.2	1.7
INT_N_1b	−0.8	−0.8	−0.1	−0.4
TS_N_1b	3.0	3.2	5.1	−3.9
INT_N_i12	−10.1	−8.6	−5.8	−7.6
TS_N_i12	−2.3	−1.7	1.6	−2.2
INT_N_2	−3.0	−2.1	0.2	−4.1
TS_N_2	−2.2	−1.8	0.7	−2.9
INT_N_3	−7.2	−6.1	−3.7	−6.7
TS_N_3	−6.1	−5.7	−3.6	−4.9
INT_N_4	−13.1	−13.2	−13.5	−12.3

[a] ZPE correction with scaling factor of 0.9877, recommended for the B3LYP/6-311G(d,p) level.[48] [b] Free energies calculated with scaling factor of 0.9877. [c] Energies calculated with PCM model, as described in Methods. [d] The energy differences are calculated based on the energy value of INT_N_1a (whose value, in hartrees, is listed in parentheses).

TABLE 5: Electronic Energy Barriers in Gas Phase (without ZPE) of the Direct and Inverse Modeled Reactivation Reactions in kcal/mol (the Highest Energy Steps of Each Reaction Are Highlighted in Red)

direct reactivation reaction					
	oximate	enolate	peroxile	hydrazonate	sulfenate
TS_1	5.5	4.1	4.3	1.8	4.5
TS_i12	X	3.8	3.3	7.8	3.8
TS_2	0.1	1.8	0.1	0.8	1.1
TS_3	2.9	2.9	2.4	1.1	2.1
inverse reactivation reaction					
	oximate	enolate	peroxile	hydrazonate	sulfenate
TS_1	4.7	5.5	14.0	11.9	7.5
TS_i12	X	0.1	0.1	0.7	0.1
TS_2	1.0	1.9	1.4	5.0	0.6
TS_3	5.4	5.2	4.4	7.0	5.9

TABLE 6: Electronic Energy Barriers in Gas Phase (with ZPE) of the Direct and Inverse Modeled Reactivation Reactions, in kcal/mol (the Highest Energy Steps of Each Reaction Are Highlighted in Red)

direct reactivation reaction					
	oximate	enolate	peroxile	hydrazonate	sulfenate
TS_1	5.7	4.2	4.1	2.0	4.6
TS_i12	X	3.4	2.9	6.9	3.2
TS_2	−0.1	1.4	0.0	0.3	0.8
TS_3	1.9	2.1	1.4	0.4	1.1
inverse reactivation reaction					
	oximate	enolate	peroxile	hydrazonate	sulfenate
TS_1	4.4	4.5	12.7	10.6	6.9
TS_i12	X	−0.1	0.0	0.4	−0.1
TS_2	0.8	1.7	1.4	4.3	0.4
TS_3	5.6	5.4	4.6	7.5	6.0

TABLE 7: Electronic Energy Barriers in Water (PCM Model) of the Direct and Inverse Modeled Reactivation Reactions, in kcal/mol (the Highest Energy Steps of Each Reaction Are Highlighted in Red)

direct reactivation reaction					
	oximate	enolate	peroxile	hydrazonate	sulfenate
TS_1	4.1	4.8	4.0	1.7	4.3
TS_i12	X	2.7	2.4	5.4	2.7
TS_2	1.7	2.4	0.3	1.2	1.4
TS_3	5.9	5.7	4.9	1.8	4.4
inverse reactivation reaction					
	oximate	enolate	peroxile	hydrazonate	sulfenate
TS_1	3.0	0.7	8.8	9.3	3.3
TS_i12	X	1.2	0.7	1.9	0.9
TS_2	1.6	2.5	1.3	3.8	1.0
TS_3	4.3	4.8	3.2	7.4	5.3

TABLE 8: Gibbs Free Energy Barriers in Gas Phase at 298.15 K and 1.0 atm of the Direct and Inverse Modeled Reactivation Reactions in kcal/mol (the Highest Energy Steps of Each Reaction Are Highlighted in Red)

direct reactivation reaction					
	oximate	enolate	peroxile	hydrazonate	sulfenate
TS_1	6.4	6.2	4.8	4.2	6.4
TS_i12	X	3.9	4.2	7.4	4.0
TS_2	0.5	2.3	0.8	0.5	1.9
TS_3	1.6	1.3	1.5	0.1	0.7
inverse reactivation reaction					
	oximate	enolate	peroxile	hydrazonate	sulfenate
TS_1	3.6	3.9	11.6	10.0	6.2
TS_i12	X	0.9	1.6	1.4	1.4
TS_2	1.5	2.4	2.6	4.4	1.5
TS_3	7.5	7.0	7.2	9.9	7.7

Tables 5 to 8 compare the electronic energy barriers in the gas phase (without and with ZPE), the electronic energy barriers in water, and the Gibbs free energy barriers of the reactivations modeled by Wang et al. in the gas phase[26] and in this work, as well as the same barriers for the inverse reactions (the rephosphylation of the serine by the phosphylated nucleophile in each case). The analysis of these tables shows that the profiles for the electronic energy barriers and the Gibbs free energy barriers are quite similar for the direct and the inverse reactions. This suggests that at least qualitatively there will be no major mistakes in considering the step with the highest electronic energy barrier as the slowest reaction step. Such procedure is largely employed, based on the fact that the electronic energy difference between the transition state and the reagents/intermediates/products is usually the most important contribution to the Gibbs free energy differences.[38] However, it should be reminded that entropic contributions are not always insignificant.

The usually given explanation for the efficiency of oximes as AChE reactivators is the existence of the α-effect in these compounds. In the theoretical models proposed in this work, a significant influence of the α-effect in the reactivation of the sarin-inhibited serine is not observed; the energetic profiles and

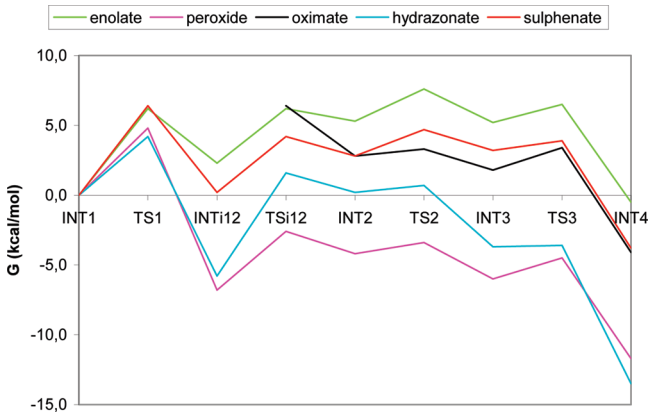

Figure 5. Gibbs free energy profiles at 298.15 K and 1.0 atm of the modeled reactivations in gas phase of the sarin-serine adduct by the formoximate and the four nucleophiles of this work, obtained by B3LYP/6-311G(d,p). For the formoximate (black line), the TS_i12 and INT_i12 entities do not exist.

the highest energy barriers for the direct reactions of reactivation by the enolate (which does not present an α-effect) and by the other nucleophiles (which do present an α-effect) do not show significant differences. For instance, when considering the free energy differences in the gas phase, it is observed that only the methylperoxile has a considerably lower highest energy barrier (4.8 kcal/mol); with the other reactivators, the highest energy barrier varies from 6.2 to 7.4 kcal/mol. When considering the electronic energy differences in water, all five reactivators have the highest barrier values between 4.4 and 5.9 kcal/mol. In this way, one can conclude that, according to the data of Wang and co-workers[26] and to our models, the α-effect is not an essential factor for the nonenzymatic reactivation of sarin-inhibited serine. To calculate accurately the α-effect, it is necessary to have a similar Ka between the compared α- and normal nucleophiles. However, this type of effect has been often carried out with nucleophiles with very different basicity.[49] Accordingly, our conclusions regarding the role of the α-effect of the nucleophiles on the dephosphylation reactions are qualitatively supported.

However, an interesting fact is observed when it is also considered the possibility of occurrence of the inverse reaction (the reinhibition by the phosphonilated nucleophile), whose energy barriers are also listed on Tables 5 to 8. For the oximate and the enolate, the highest energy barriers are nearly the same for the direct and the inverse reactions; in some cases, such as the models for reactions in water, the inverse reaction barriers are lower than those for the direct reaction. In the case of reactivation by the sulfenate, the highest electronic energy barriers in gas phase for the inverse reaction are significantly larger than those for the direct reaction; in water, this difference is reduced, being the barrier for the direct reaction 0.9 kcal/mol lower than that for the inverse reaction. In terms of Gibbs free energy, the barrier for the direct reaction is 1.3 kcal/mol lower than for the inverse reaction. For the peroxile and the hydrazonate, the barriers for the direct reaction are always substantially lower than those for the inverse reaction. This fact may constitute an advantage for the action of these compounds as reactivators of the inhibited serine, even considering that in absolute values the barriers for the direct reaction of the formaldehyde hydrazonate in the gas phase are a bit larger than those calculated for the other nucleophiles.

Another interesting result is obtained from the analysis of the Gibbs free energy profiles for the reactivations by the five nucleophiles, shown in Figure 5. The final products of the reactivations by methylperoxile and by formaldehyde hydrazonate (INT_4) are more than 10.0 kcal/mol more stable than the initial reagents (INT_1). For reactivations by formoximate and by methylsulfenate, this difference is about 3.5 kcal/mol. Finally, for the enolate of acetaldehyde, this difference is only 0.5 kcal/mol. These data show that the final products of the modeled reactivations by the peroxile, the hydrazonate and, to a lesser extent, by the sulfenate and by the oximate, are more stable than the initial reagents. In all cases, the barriers for the first step of the inverse reaction (corresponding to TS_3) are relatively high, being all larger than 7.0 kcal/mol.

Peroxiles and sulfenates as well as enolates are usually very unstable in physiological conditions, and their use as antidotes for neurotoxic agents is very unlikely. However, hydrazones are much more stable, and some of them could be converted to hydrazonates at physiological pH. Additional in vitro and in vivo experimental studies should determine if hydrazones can be used as AChE reactivators, estimating the viability of their use as antidotes against intoxications by sarin and other neurotoxic agents, as well as against intoxications by organophosphorus insecticides.

It is noteworthy that reactivation by formoximate was the only one whose modeled reaction shows a three-step mechanism. Although a reaction rate is limited by its slowest step (the one with the highest activation energy), it is possible that the reactivation by formoximate, possessing only three steps, may have a significant advantage when compared to the other modeled nucleophiles.

The proposed models do not give any clue about the reasons of the mechanism differences among the five nucleophiles. The comparison of atomic charges, bond orders, and internuclear distance data between some of the main atoms of the studied complexes show little differences among them: only the charge of the nucleophilic atom and the distance between this and the phosphorus atom in the several minima INT_1 vary considerably from one nucleophile to another (data not shown). There were no significant differences of these parameters when comparing the energy data and the populational analysis in the gas phase and in water (which is not surprising, since the energy calculations in water were done with the geometries minimized in the gas phase). However, it is evident the need of a precise reactivator orientation at the beginning of the reaction. In each studied case, the nucleophile adopted a characteristic orientation in the minimum INT_1 and in the transition state TS_1, and in the particular case of the formaldehyde hydrazonate the two modeled reaction pathways differed between them in the orientation of the nucleophile in those steps. These results indicate that the correct orientation of the antidote is not necessary only for enzymatic reactivations, caused by some spatial constraint inside the active site gorge of AChE, but it is an intrinsic requirement of the reaction, as observed in all the models of the studied nonenzymatic reactivations. More studies are needed to clarify why each nucleophile adopts a specific orientation.

The modeled reactions are hypothetical nonenzymatic reactivations of an isolated serine inhibited by sarin analogues. In the real problem, the inhibited serine is an essential component of the active site of AChE. Several references have shown that many other AChE residues take part in the catalysis process.[50−71] In this way, we cannot guarantee a priori that hydrazonates would be efficient reactivators for inhibited AChE, since it is not proven yet that these compounds are able to reach and reactivate the serine in the bottom of the active site gorge. However, we believe that the present work shows that it is

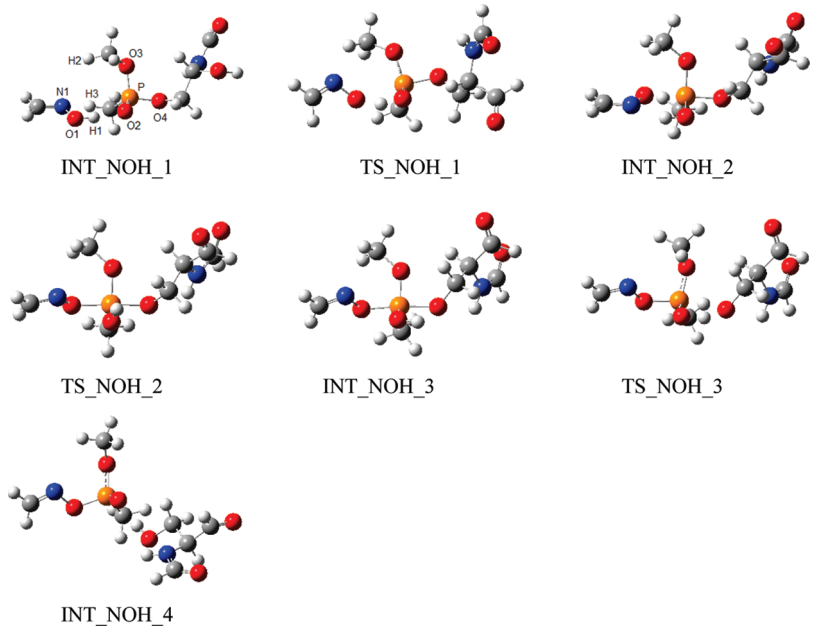

Figure 6. Structures of the minima (INT_NOH) and transition states (TS_NOH) of the potential energy surface of the modeled sarin-serine adduct reactivated by formoxime, obtained by B3LYP/6-311G(d,p) (C in gray, O in red, N in blue, P in orange, and H in white).

TABLE 9: Energies for Minima and Transition States of the Sarin-Serine Adduct Reactivation by Formoxime at the B3LYP/6-311G(d,p) Level (kcal/mol)

structures	ΔE (without ZPE)[a]	ΔE (with ZPE)[a]	ΔG^0 (298.15 K)[b]	ΔE_{PCM}[c]
INT_NOH_1[d]	0.0 (−1178.23952)	0.0 (−1178.00292)	0.0 (−1178.05756)	0.0 (−1178.26667)
TS_NOH_1	36.0	34.7	37.0	36.2
INT_NOH_2	17.9	18.7	22.0	20.7
TS_NOH_2	31.6	30.9	33.6	29.8
INT_NOH_3	25.4	25.7	28.8	24.6
TS_NOH_3	37.0	35.0	37.9	38.4
INT_NOH_4	4.4	3.9	1.9	3.8

[a] ZPE correction factor with scaling factor of 0.9877, recommended for the B3LYP/6-311G(d,p) level.[48] [b] Free energies calculated with scaling factor of 0.9877. [c] Energies calculated with PCM model, as described in Methods. [d] The energy differences are calculated based on the energy value of INT_NOH_1 (whose value, in hartrees, is listed in parentheses).

worthy to further evaluate this possibility, since it could open a whole new branch in the treatment of intoxication by organophosphorus compounds.

Finally, we have also applied the same procedure to model the reactivation by neutral formoxime in order to answer the question about which is the preferred form of the nucleophile for the reaction, the deprotonated[32] or the neutral one.[33] The obtained structures are shown in Figure 6, and the energetic profiles for the reactions are listed in Table 9.

As can be seen in Figure 6 and analogously to the formoximate anion, the reactivation by the neutral formoxime is a three-step mechanism. The first step involves the transition state TS_NOH_1, whose only imaginary frequency (211i cm^{-1}) possesses a vibrational mode corresponding to a nucleophilic attack of the oxime to the phosphylated serine, concerted with the transfer of the H1 proton from the O1 atom to the O2 atom. The second step consists of a rotation of the P−O2 bond in such a way that the H1 atom orients itself toward the serine; this movement corresponds to the vibrational mode of the only imaginary frequency of the transition state TS_NOH_2 (486i cm^{-1}). Finally, the last step involves the transition state TS_NOH_3, whose imaginary frequency is 439i cm^{-1}; its vibrational mode corresponds to a transfer of the H1 proton from O2 to O4, concerted with the elimination of the serine. Table 9 shows that in the gas phase and in aqueous solution, the first step is the one with the highest electronic energy barriers. In the gas phase, this barrier corresponds to 36.0 kcal/mol (34.7 kcal/mol with ZPE) and in water to 36.2 kcal/mol. The first step is also the one with the highest Gibbs free energy barrier in the gas phase (37.0 kcal/mol at 298.15 K and 1.0 atm). It is interesting that, unlike all the anionic nucleophiles modeled in this work, there are no major differences between the energetic profiles in the gas phase and in water for the oxime.

Comparing the energetic profiles of the formoxime reaction with that of formoximate,[26] it is observed that the energy barriers for the reactivation by the latter are much lower than those for the neutral reactivator. For instance, at 298.15 K and 1.0 atm, the activation free energy for the formoximate equals 6.4 kcal/mol, while for the formoxime its value is 37.0 kcal/mol (nearly six times higher). One can conclude that, at least for the nonenzymatic reactivation by oximes, the reaction is faster for the deprotonated form of the oxime than for the neutral one. Such conclusion reinforces the generally accepted hypothesis for reactivation by oximes at the AChE active site and seems to discard the idea previously proposed by our workgroup.[33] Our new model does not explain why the energy barriers are so much higher for the neutral oxime. However, we can hypothesize that the requirements of quite different orientations of the oxime (when compared to the deprotonated form) at the beginning of the reaction, and of the serine at the end, caused

by the need of transference of the H1 proton, prevents the formoxime from adopting an optimal orientation for the reaction; this problem would not occur with the formoximate. Another previous work of our group[72] has shown that cationic oximes can access AChE active site better than the neutral ones and much better than the anionic ones, indicating that the deprotonation of the oximes should happen inside the enzyme active site, just before the reactivation process.

As pointed out by one of the referees, it is also possible that the reason for the higher efficiency of the oximes lies on their deprotonation. Since this work indicates that the deprotonated form of the oxime is actually involved in AChE reactivation, one may hypothesize that if the same is true for the other nucleophiles modeled in this work perhaps their deprotonations by a basic residue at the enzyme active site are not so easy. If this is true, the differences on the reactivation power between different nucleophiles would be due to their different deprotonation behavior inside AChE.

Finally, it is important to note that the phosphonylation of serine modeled by Wang et al.[25] gave quite similar results; the energetic barriers for inhibition of the neutral serine (which acts as nucleophile in this case) are much higher than those for the inhibition of the deprotonated serine.

The use of basis sets with diffuse functions is known to be more appropriate to model anions and atoms with isolated electronic pairs. In order to evaluate if the lack of diffuse functions in our models could compromise our conclusions, we have performed single point energy calculations in all stationary points described in this work with the B3LYP/6-311+G(d,p) level of theory. The results show that, although there are some quantitative differences between the energy barriers calculated with the 6-311G(d,p) and the 6-311+G(d,p) basis sets, there is no major qualitative difference; the profiles of electronic energy in gas phase and in water calculated with these two models are approximately parallel. A table with energies calculated with the B3LYP/6-311+G(d,p) level of theory and figures comparing the profiles obtained with the two models are available in the Supporting Information.

Conclusion

The reaction pathways of the reactivation of a sarin-serine adduct model by different nucleophiles have been modeled, using the B3LYP/6-311G(d,p) level of theory and confirmed with single point B3LYP/6-311+G(d,p) calculations. Our models show that each nucleophile reactivates the sarin-inhibited serine by very similar mechanisms, which are distinguished mainly by the orientation of the antidote in the first step of the reaction. Formoximate has previously been shown to react in only three steps, while the other nucleophiles modeled in this work react in four steps. Formaldehyde hydrazonate reactivates the serine in a slight different manner with two possible pathways and a second step different from that modeled for the other reactivators. The calculated energetic profiles suggest that the nucleophile α-effect is not important for dephosphylation reactions and the possibility of using hydrazones, peroxiles and, to a lesser extent, sulfenates for the reactivation of sarin-inhibited AChE, although in principle only the hydrazones are stable enough to be of practical use. Experimental studies will be conducted to evaluate this possibility.

The reaction pathway of the reactivation of the same adduct by the neutral formoxime has also been modeled, and the comparison of its energetic profile with that of the reactivation by the deprotonated formoxime indicates that the latter is indeed the preferred form for the nonenzymatic reaction.

Acknowledgment. We gratefully acknowledge the Brazilian Ministry of Defense and CAPES (Pro-defesa), CNPq, and $IMBEB_2$ for financial support. We are also grateful to Dr. Jerzy Leszczynski from Jackson State University for kindly providing the coordinates of one of the structures of his work, allowing us to reproduce it as a benchmark for our own work.

Supporting Information Available: Cartesian coordinates for all structures modeled in this work, a table with energies calculated with the B3LYP/6-311+G(d,p) level of theory, and figures comparing the profiles obtained with the 6-311G(d,p) and the 6-311+G(d,p) basis sets. This material is available free of charge via the Internet at http://pubs.acs.org.

References and Notes

(1) Quinn, D. M. *Chem. Rev.* **1987**, *87*, 955–979.
(2) Taylor, P. *J. Biol. Chem.* **1991**, *266*, 4025–4028.
(3) MacPhee-Quigley, K.; Taylor, P; Taylor, S. *J. Biol. Chem.* **1985**, *260*, 12185–12189.
(4) Schumacher, M.; Camp, S.; Maulet, Y.; Newton, M.; MacPhee-Quigley, K; Taylor, S. S.; Friedmann, T; Taylor, P. *Nature* **1986**, *319*, 407–409.
(5) Gibney, G.; Camp, S.; Dionne, M.; MacPhee-Quigley, K; Taylor, P. *Proc. Natl. Acad. Sci. U.S.A.* **1990**, *87*, 7546–7550.
(6) Sussman, J. L.; Harel, M.; Frolow, F.; Oefner, C.; Goldman, A.; Toker, L.; Silman, I. *Science* **1991**, *253*, 872–879.
(7) Shafferman, A.; Kronman, C.; Flashner, Y.; Leitner, M.; Grosfeld, H.; Ordentlich, A.; Gozes, Y.; Cohen, S.; Ariel, N.; Barak, D.; Harel, M.; Silman, I.; Sussman, J. L.; Velan, B. *J. Biol. Chem.* **1992**, *267*, 17640–17648.
(8) Fukuto, T. R. *Environ. Health Perspect.* **1990**, *87*, 245–254.
(9) Kwong, T. C. *Ther. Drug Monit.* **2002**, *24*, 144–149.
(10) Worek, F.; Thiermann, H.; Szinicz, L.; Eyer, P. *Biochem. Pharmacol.* **2004**, *68*, 2237–2248.
(11) Majumdar, D.; Roszak, S.; Leszczynski, J. *J. Phys. Chem. B* **2006**, *110*, 13597–13607.
(12) Marrs, T. C. In *Chemical Warfare Agents - Toxicology and Treatment*, 2nd ed.; Marrs, T. C., Maynard, R. L, Sidell, F. R., Eds.; John Wiley & Sons Ltd: West Sussex, England, 2007; pp 191−221.
(13) Moretto, A *Toxicol. Lett.* **1998**, *102*−*103*, 509–513.
(14) Gupta, R. C. In *Toxicology of Organophosphate & Carbamate Compounds*, 1a ed.; Gupta, R. C., Ed.; Elsevier Academic Press: London, 2006; pp 5−24.
(15) *UN Report S/16433*; United Nations: New York, 1984.
(16) *UN Report S/117911*; United Nations: New York, 1986.
(17) MacIlwain, C. *Nature* **1993**, *363*, 3.
(18) Nagao, M.; Takatori, T.; Matsuda, Y.; Nakajima, M.; Iwase, H.; Iwadate, K. *Toxicol. Appl. Pharmacol.* **1997**, *144*, 198.
(19) Sidell, F. R. In *Medical Aspects of Chemical and Biological Warfare - Textbook of Military Medicine*; Sidell, F. R., Takafuji, E. T., Franz, D. R., Eds.; Office of the Surgeon General, U.S. Army: Washington D.C., 1997; pp 129−179.
(20) Yanagisawa, N.; Morita, H. *J. Neurol. Sci.* **2005**, *238*, S81.
(21) Yanagisawa, N.; Morita, H.; Nakajima, T. *J. Neurol. Sci.* **2006**, *249*, 76.
(22) Yokoyama, K. *Neurotoxicology* **2007**, *28*, 364.
(23) Nozaki, H.; Aikawa, N.; Fujishima, S.; Suzuki, M.; Shinozawa, Y.; Hori, S.; Nogaws, S. *Lancet* **1995**, *346*, 698.
(24) Cannard, K. *J. Neurol. Sci.* **2006**, *249*, 86–94.
(25) Wang, J.; Gu, J.; Leszczynski, J. *J. Phys. Chem. B* **2006**, *110*, 7567–7573.
(26) Wang, J.; Gu, J.; Leszczynski, J.; Feliks, M.; Sokalski, W. A. *J. Phys. Chem. B* **2007**, *111*, 2404–2408.
(27) Wang, J.; Gu, J.; Leszczynski, J. *J. Phys. Chem. B* **2008**, *112*, 3485–3494.
(28) Kassa, J. *J. Toxicol. - Clin. Toxicol.* **2002**, *40*, 803–816.
(29) Kuca, K.; Jun, D.; Musilek, K. *Mini-Rev. Med. Chem.* **2006**, *6*, 269–277.
(30) March, J. *Advanced Organic Chemistry: Reactions, Mechanisms, and Structure*, 4th ed.; John Wiley & Sons Inc.: New York, 1992.
(31) Tarkka, R. M.; Buncel, E. *J. Am. Chem. Soc.* **1995**, *117*, 1503–1507.
(32) Ashani, Y.; Radic, Z.; Tsigelny, I.; Vellom, D. C.; Pickering, N. A.; Quinn, D. M.; Doctor, B. P; Taylor, P. *J. Biol. Chem.* **1995**, *270*, 6370–6380.
(33) Castro, A. T; Figueroa-Villar, J. D. *Int. J. Quantum Chem.* **2002**, *89*, 135–146.
(34) Becke, A. D. *J. Chem. Phys.* **1993**, *98*, 5648–5652.
(35) Lee, C.; Yang, W.; Parr, R. G. *Phys. Rev. B* **1988**, *37*, 785–789.

(36) Miehlich, B.; Savin, A.; Stoll, H.; Preuss, H. *Chem. Phys. Lett.* **1989**, *157*, 200–206.
(37) Leach, A. R. *Molecular Modelling: Principles and Applications*, 2nd ed.; Pearson Educated Limited: Essex, England, 2001.
(38) Jensen, F. *Introduction to Computational Chemistry*, 2nd ed.; John Wiley & Sons Ltd.: Chichester, England, 2007.
(39) Reed, A. E.; Curtiss, L. A.; Weinhold, F. *Chem. Rev.* **1988**, *88*, 899–926.
(40) Cossi, M.; Barone, V.; Cammi, R.; Tomasi, J. *Chem. Phys. Lett.* **1996**, *255*, 327–335.
(41) Cancès, E.; Mennucci, B.; Tomasi, J. *J. Chem. Phys.* **1997**, *107*, 3032–3041.
(42) Mennucci, B.; Tomasi, J. *J. Chem. Phys.* **1997**, *106*, 5151–5158.
(43) Cossi, M.; Barone, V.; Mennucci, B.; Tomasi, J. *Chem. Phys. Lett.* **1998**, *286*, 253–260.
(44) Cossi, M.; Scalmani, G.; Rega, N.; Barone, V. *J. Chem. Phys.* **2002**, *117*, 43–54.
(45) Florián, J.; Warshel, A. *J. Phys. Chem. B* **1998**, *102*, 719–734.
(46) Seckuté, J.; Menke, J. L.; Emnett, R. J.; Patterson, E. V.; Cramer, C. J. *J. Org. Chem.* **2005**, *70*, 8649–8660.
(47) Frisch, M. J.; Trucks, G. W.; Schlegel, H. B.; Scuseria, G. E.; Robb, M. A.; Cheeseman, J. R.; Montgomery Jr., J. A.; Vreven, T.; Kudin, K. N.; Burant, J. C.; Millam, J. M.; Iyengar, S. S.; Tomasi, J.; Barone, V.; Mennucci, B.; Cossi, M.; Scalmani, G.; Rega, N.; Petersson, G. A.; Nakatsuji, H.; Hada, M.; Ehara, M.; Toyota, K.; Fukuda, R.; Hasegawa, J.; Ishida, M.; Nakajima, T.; Honda, Y.; Kitao, O.; Nakai, H.; Klene, M.; Li, X.; Knox, J. E.; Hratchian, H. P.; Cross, J. B.; Bakken, V.; Adamo, C.; Jaramillo, J.; Gomperts, R.; Stratmann, R. E.; Yazyev, O.; Austin, A. J; Cammi, R.; Pomelli, C.; Ochterski, J. W.; Ayala, P. Y.; Morokuma, K.; Voth, G. A.; Salvador, P.; Dannenberg, J. J.; Zakrzewski, V. G.; Dapprich, S. ; Daniels, A. D. ; Strain, M. C. ; Farkas, O. ; Malick, D. K. ; Rabuck, A. D. ; Raghavachari, K. ; Foresman, J. B.; Ortiz, J. V.; Cui, Q.; Baboul, A. G.; Clifford, S.; Cioslowski, J.; Stefanov, B. B.; Liu, G.; Liashenko, A.; Piskorz, P.; Komaromi, I.; Martin, R. L.; Fox, D. J.; Keith, T.; Al-Laham, M. A.; Peng, C. Y.; Nanayakkara, A.; Challacombe, M.; Gill, P. M. W.; Johnson, B.; Chen, W.; Wong, M. W.; Gonzalez, C.; Pople, J. A. *Gaussian 03*, rev D.01; Gaussian, Inc.: Wallingford, CT, 2004.
(48) Andersson, M. P.; Uvdal, P. *J. Phys. Chem. A* **2005**, *109*, 2937–2941.
(49) Buncel, E.; Um, I.-H. *Tetrahedron* **2004**, *60*, 7801–7825.
(50) Sussman, J. L.; Harel, M.; Frolow, F.; Oefner, C.; Goldman, A.; Toker, L.; Silman, I. *Science* **1991**, *253*, 872–879.
(51) Harel, M.; Schalk, I.; Ehret-Sabatier, L.; Bouet, F.; Goeldner, M.; Hirth, C.; Axelsen, P. H.; Silman, I.; Sussman, J. L. *Proc. Natl. Acad. Sci. U.S.A.* **1993**, *90*, 9031–9035.
(52) Ripoll, D. R.; Faerman, C. H.; Axelsen, P. H.; Silman, I.; Sussman, J. L. *Proc. Natl. Acad. Sci. U.S.A.* **1993**, *90*, 5128–5132.
(53) Selwood, T.; Feaster, S. R.; States, M. J.; Pryor, A. N.; Quinn, D. M. *J. Am. Chem. Soc.* **1993**, *115*, 10477–10482.
(54) Tan, R. C.; Truong, T. N.; McCammon, J. A.; Sussman, J. L. *Biochemistry* **1993**, *32*, 401–403.
(55) Vellom, D. C.; Radic, Z.; Li, Y.; Pickering, N. A.; Camp, S.; Taylor, P. *Biochemistry* **1993**, *32*, 12–17.
(56) Axelsen, P. H.; Harel, M.; Silman, I.; Sussman, J. L. *Protein Sci.* **1994**, *3*, 188–197.
(57) Hosea, N. A.; Berman, H. A.; Taylor, P. *Biochemistry* **1995**, *34*, 11528–11536.
(58) Harel, M.; Quinn, D. M.; Nair, H. K.; Silman, I.; Sussman, J. L. *J. Am. Chem. Soc.* **1996**, *118*, 2340–2346.
(59) Dodson, G.; Wlodawer, A. *Trends Biochem. Sci.* **1998**, *23*, 347–352.
(60) Enyedy, I. J.; Kovach, I. M.; Brooks, B. R. *J. Am. Chem. Soc.* **1998**, *120*, 8043–8050.
(61) Fuxreiter, M.; Warshel, A. *J. Am. Chem. Soc.* **1998**, *120*, 183–194.
(62) Botti, S. A.; Felder, C. E.; Lifson, S.; Sussman, J. L.; Silman, I. *Biophys. J.* **1999**, *77*, 2430–2450.
(63) Taylor, P.; Wong, L.; Radic, Z.; Tsigelny, I.; Brüggemann, R.; Hosea, N. A.; Berman, H. A. *Chem.-Biol. Interact.* **1999**, *119*−*120*, 3–15.
(64) Wong, L.; Radic, Z.; Brüggemann, R. J. M.; Hosea, N.; Berman, H. A.; Taylor, P. *Biochemistry* **2000**, *39*, 5750–5757.
(65) Barak, D.; Kaplan, D.; Ordentlich, A.; Ariel, N.; Velan, B.; Shafferman, A. *Biochemistry* **2002**, *41*, 8245–8252.
(66) Zhang, Y.; Kua, J.; McCammon, J. A. *J. Am. Chem. Soc.* **2002**, *124*, 10572–10577.
(67) Kaplan, D.; Barak, D.; Ordentlich, A.; Kronman, C.; Velan, B.; Shafferman, A. *Biochemistry* **2004**, *43*, 3129–3136.
(68) Ordentlich, A.; Barak, D.; Sod-Moriah, G.; Kaplan, D.; Mizrahi, D.; Segall, Y.; Kronman, C.; Karton, Y.; Lazar, A.; Marcus, D.; Velan, B.; Shafferman, A. *Biochemistry* **2004**, *43*, 11255–11265.
(69) Shafferman, A.; Barak, D.; Kaplan, D.; Ordentlich, A.; Kronman, C.; Velan, B. *Chem.-Biol.Interact* **2005**, *157*−*158*, 123–131.
(70) Sant'anna, C. M. R.; Viana, A. S.; Junior, N. M. N. *Bioorg. Chem.* **2006**, *34*, 77–89.
(71) Nemukhin, A. V.; Lushchekina, S. V.; Bochenkova, A. V.; Golubeva, A. A.; Varfolomeev, S. D. *J. Mol. Model.* **2008**, *14*, 409–416.
(72) Gonçalves, A. S.; França, T. C. C.; Silva, A. W. S.; Figueroa-Villar, J. D. *J. Braz. Chem. Soc.* **2006**, *17*, 968–975.

JP810686K